RESEARCH ARTICLE | DECEMBER 02 2016

Direct fabrication of compound-eye microlens array on curved surfaces by a facile femtosecond laser enhanced wet etching process

Hao Bian; Yang Wei; Qing Yang; ... et. al

Appl. Phys. Lett. 109, 221109 (2016)
https://doi.org/10.1063/1.4971334

Direct fabrication of compound-eye microlens array on curved surfaces by a facile femtosecond laser enhanced wet etching process

Hao Bian, Yang Wei, Qing Yang,[a] Feng Chen,[a] Fan Zhang, Guangqing Du, Jiale Yong, and Xun Hou

State Key Laboratory for Manufacturing System Engineering and Shaanxi Key Laboratory of Photonics Technology for Information, Xi'an Jiaotong University, Xi'an 710049, People's Republic of China

(Received 29 August 2016; accepted 19 November 2016; published online 2 December 2016)

We report a direct fabrication of an omnidirectional negative microlens array on a curved substrate by a femtosecond laser enhanced chemical etching process, which is utilized as a molding template for duplicating bioinspired compound eyes. The femtosecond laser treatment of the curved glass substrate employs a common *x-y-z* stage without rotating the sample surface perpendicular to the laser beam, and uniform, omnidirectional-aligned negative microlenses are generated after a hydrofluoric acid etching. Using the negative microlens array on the concave glass substrate as a molding template, we fabricate an artificial compound eye with 3000 positive microlenses of 95-μm diameter close-packed on a 5-mm polymer hemisphere. Compared to the transferring process, the negative microlenses directly fabricated on the curved mold by our method are distortion-free, and the duplicated artificial eye presents clear and uniform imaging capabilities. This work provides a facile and efficient route to the fabrication of microlenses on any curved substrates without complicated alignment and motion control processes, which has the potential for the development of new microlens-based devices and systems. *Published by AIP Publishing*. [http://dx.doi.org/10.1063/1.4971334]

Curved microlens arrays inspired by the insect compound eyes are considered as ideal view vision systems with advantages of miniaturization, multi-aperture, and large field-of-view (FOV), presenting their essential applications in wide-view-angle imaging, fast motion detection, and other demanding applications.[1–3] Currently, fabrication of microlenses or micro-optical elements on curved substrates is mainly achieved by means of transferring or bending methods based on planar manufacturing technologies.[4–11] During the transferring or bending process when a flat microlens array is deformed into a 3D curved geometry, distortions of individual lenslets would inevitably be induced by non-uniform distribution of strain forces on different parts of the microlens array, which will severely degrade the performance of the device. To obtain high-quality curved microlens arrays without distortions, the best solution is to fabricate microlenses directly on curved substrates. However, existing technologies for the curved-substrate manufacturing heavily rely on expensive high-precision multi-axis platforms that usually integrate several linear and rotation stages, and corresponding complex motion control and low-efficiency tool paths,[12–14] which is not practical for the fabrication of compound eye microlenses that consist of thousands of lenslets.

In pursuit of a low-cost, high-efficient approach to the direct fabrication of microlenses on curved substrates, we look into the femtosecond laser enhanced chemical etching process, which has been proved to be a powerful tool to generate large-area, uniform microlens arrays with excellent optical performances.[15–17] Different from the previous post-bending method to form curved microlens arrays,[11,18] here we present a facile route to directly fabricate microlenses with controllable size, high consistency, and zero distortions on a concave glass substrate. Bioinspired compound-eye microlens arrays can be obtained by a reverse molding process. Because it is not necessary to direct the laser beam along the normal direction of the curved surface, complex multi-axis motion control is not needed in our method. The femtosecond laser treatment is accomplished by a common *x-y-z* linear stage, but omnidirectional negative spherical microlenses with uniform and smooth spherical surfaces can be obtained on the concave hemispherical glass substrate after a high-efficient hydrofluoric acid (HF) etching.

The fabrication process of the curved microlens array is divided into two main steps, as illustrated in Fig. 1. First, the concave glass mold with negative microlenses is fabricated by the femtosecond laser enhanced chemical etching process. A spherical plano-concave lens with a diameter of 6 mm (K-9 glass; focal length is 6 mm) was used as the curved substrate in the experiment. The lens is fixed on a 3D stage with only *x-y-z* linear stage (M-505.2DG, Physik Instrumente). The femtosecond laser (800 nm, 50 fs, 1 kHz) is initially focused on the center of the concave surface of the lens in normal irradiation by a microscope objective lens (Nikon, N.A. = 0.5), and the power of the laser is 3 mW. A breakdown-induced crater can be created by a 0.5-s exposure, which is controlled by a mechanical shutter. Then, the lens is translated to the next point. In this manner, a hexagonal-packed array of the laser exposure spots can be fabricated. The position of the *z*-axis is individually adjusted before each laser exposure, ensuring that the curved sample surface is on focus during the entire process. We do not need to rotate the sample, so the angle between the laser incident direction and the normal direction of the curved surface varies from 0° to 40° at different positions. After the laser exposures, the lens is immersed in the HF (10%) ultrasound bath for 80 min.

[a]Authors to whom correspondence should be addressed. Electronic addresses: yangqing@mail.xjtu.edu.cn and chenfeng@mail.xjtu.edu.cn.

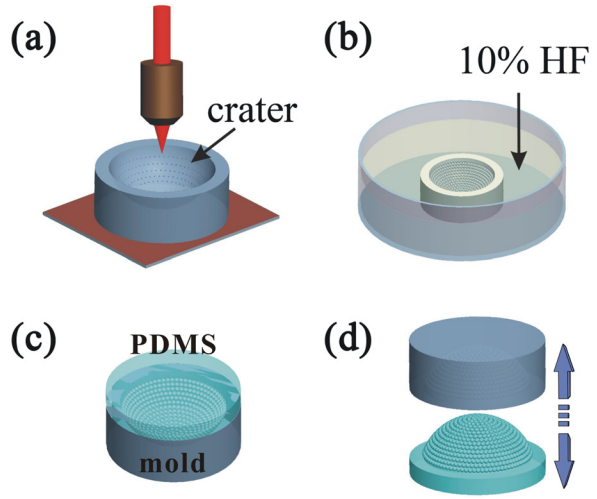

FIG. 1. Schematic illustration of the fabrication process of the compound eye inspired curved microlens array. (a) Femtosecond laser point-by-point exposures on the curved lens. (b) 10% HF solution ultrasonic bath for the wet etching process to produce concave microlens array-in-lens. (c) PDMS pouring and solidifying. (d) Peeling replication mold and obtain an artificial compound eye.

Isotropic chemical etching in the laser-induced craters eventually forms concave spherical microstructures on the curved surface of the concave lens (Fig. S1, supplementary material). The second step is to replicate compound eye microlens arrays on a polydimethylsiloxane (PDMS) dome from the concave lens with negative microlenses, as shown in Figs. 1(c) and 1(d). The PDMS pre-polymer is prepared by mixing the Dow Corning Sylgard 184 and the catalyst with the ratio of 10:1 and degassing in a vacuum for 1 h. After pouring the liquid polymer into the concave lens followed by a peeling process, the compound eye inspired curved microlens array is fabricated after the de-molding process.

Figures 2(a) and 2(b) show the SEM observations of the compound eye inspired curved microlens array. The microlens array consists of 3000 lenslets, which are uniformly distributed on the PDMS dome with a diameter of 6 mm. A magnified observation in Fig. 2(b) demonstrates 100% fill factor of the microlenses with hexagonal profiles. The diameter of each microlens is about 95 μm. Such a dimension and an alignment pattern of the microlenses are comparable to the ommatidia of natural compound eyes, which show great potential in developing compound eye inspired optical devices. The microlenses on the PDMS dome are highly uniform, as demonstrated in Fig. 2(b), and no shape distortions can be found in the SEM images, indicating the capability of our method, which can fabricate high-quality microlenses directly on the curved substrate.

We investigate the 3D morphology of a few microlenses on the top and side of curved microlens array by a laser scanning confocal microscope (LCSM, Olympus LEXT OLS4000). The results are shown in Figs. 2(c) and 2(d), respectively. Fig. 2(e) shows the cross-sectional profile of the microlens on the artificial compound eyes as marked in Fig. 2(c). The two segment dotted line as shown in Fig. 2(c), which is the theoretically fitting of the parabola, demonstrates that the profile of the lenslets can be identified as a parabola. After measuring the geometrical size of the compound eye inspired

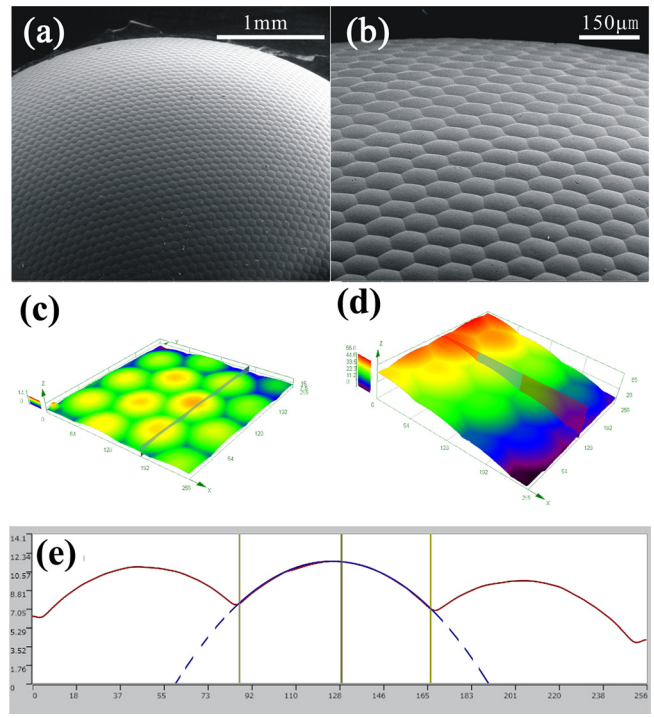

FIG. 2. (a), (b) SEM images of the 45° SEM observation of the compound eye inspired curved microlens array. (c) and (d) 3D morphology of microlenses on the top and side of the compound eye. (e) The cross-sectional profile of the microlenses as marked in (c). The dotted line is the ideal parabola line.

microlens array at different areas, the diameters of the ommatidia range from 93.18 μm to 96.18 μm and the average sag height is 4.58 μm. The deformation ratio of the diameters is calculated as 2.96%, which demonstrates the relatively high fidelity of the microlens array.[11] The size deformation of the microlenses generally comes from different angles between the laser incident direction and the normal direction of the curved surface at different positions, which would be discussed later. The manually ensured focus condition of the focused laser pulse to the curved surface is another stumbling block, which would be overcome by a commercial mature auto-focus device. Besides, the diameters of each ommatidium could be facilely controlled from tens to hundreds of micrometers by the intensity of the femtosecond laser we used and the chemical etching parameters and the geometrical arrangement of the exposure spots.[16] Further, the average focal length of the ommatidium with a parabolic profile was calculated as[19]

$$f = \frac{D^2}{8h(n-1)}, \tag{1}$$

where D is the diameter of the ommatidium, h is the sag height of the microlens, and n is the refractive index of PDMS. With the $D = 95$ μm, $h = 4.58$ μm, and $n = 1.406$, the f will be 606.69 μm.

What's more, we used a microscope and a CCD camera to investigate the imaging performance of the compound eye inspired microlens array with a monogram *fs*, which was used as the imaging object. Figs. 3(a) and 3(b) show the equivalent and clear imaging of the monogram *fs* which formed at different focal distances. Insets in Figs. 3(a) and 3(b) are higher magnification images. Because of the geometrically spherical

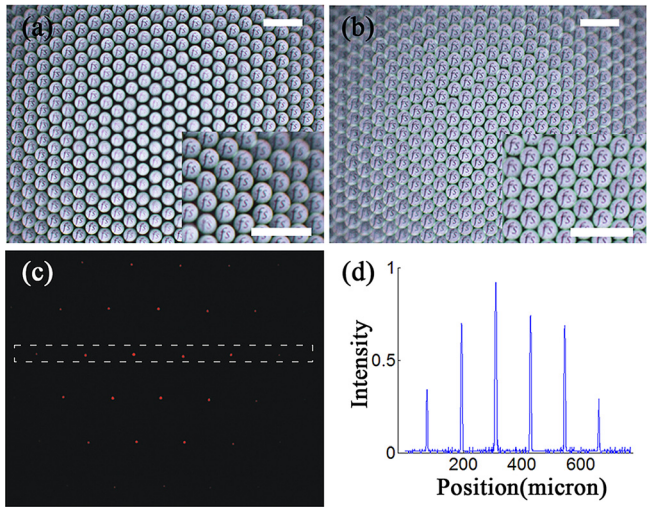

FIG. 3. (a) and (b) The imaging properties of the microlenses at different focal distances. (c) Microscopy confocal images of the compound eye illuminated by a normally incident He-Ne laser beam. (d) The intensity distribution of the focusing spots in select rectangular. Insets in panels (a) and (b) are higher magnification images of the imaging area. The scale bar in panels (a) and (b) is 200 μm.

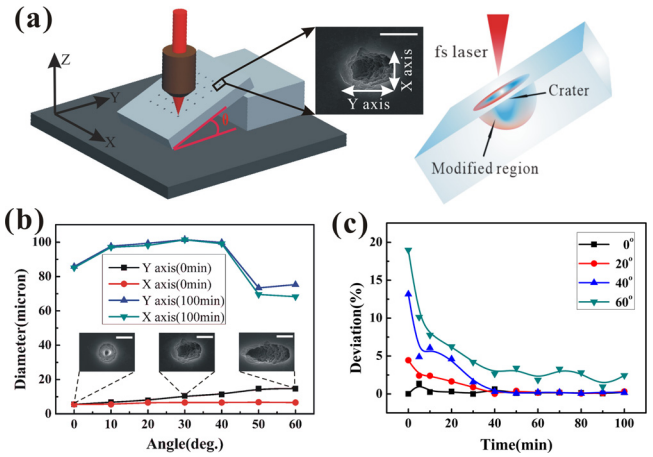

FIG. 4. (a) Schematic illustration of femtosecond laser direct writing on the inclined plane. The scale bar is 5 μm. (b) The dimensions of the structure at different tilt angles before (0 min) and after wet etch (100 min). Insets are the SEM images of the craters at different tilt angles of 0°, 30°, and 60°, respectively. The scale bar is 5 μm. (c) The variation of the microstructures via different etching times at the tilt angle of 0° and 40°.

alignment of the lenslets, the microlenses could gradually form a clear and sharp image of the monogram *fs* when changing the distance between the monogram *fs* and the microlens array as shown in the supplementary material video (S2, supplementary material). The high-quality imaging performance of the curved microlens arrays ensures their applications in microlens-based imaging and sensing devices and systems. Fig. 3(c) shows the confocal spots' imaging of the fabricated compound eyes inspired microlens array. We used a He-Ne laser beam as the light source to investigate the focusing ability of the compound eyes. Each lenslet could form a clear and circular focusing spot. The cross-sectional intensity distribution of the focusing spots in the selected rectangular area was calculated and is shown in Fig. 3(d). The sharp intensity distribution of the focusing spots demonstrates that each lenslet possesses a well focusing ability.

The facility of this method is that we do not need to rotate the curved sample to ensure the direction of the focused laser beam perpendicular to the sample surface and still can obtain uniform microlens arrays. To find the relationship between the effective incident angle of the incident laser to the sample surface and the deformation of microlenses, we simplified the fabrication process as directly focusing the femtosecond laser beam onto an inclined glass sheet under different tilt angles with the material compositions the same as the concave lens we used as the substrate. The schematic illustration of the process is shown in Fig. 4(a). We changed the tilt angle of the inclined glass sheet to simulate different efficient incident angles onto the curved surface and investigate the simultaneous morphology change of the laser ablated crater. Here, the deformation of the microlenses includes the size deviation between the microlenses and the microlens individuals. In detail, as shown in Fig. 4(a), we identify the diameters of the crater as Y (along the inclined direction) and X (perpendicular to the inclined direction) to quantify the deviation of microlens individuals as $Deviation\ (\%) = |Y - X|/((Y + X)/2)$. Fig. 4(b) shows the diameter deviation of the formed microstructures at different tilt angles before (0 min) and after HF acid etching (100 min). For the laser ablated craters before etching, with the increase of the tilt angles from 0° to 60°, the dimension of the Y axis increases at the same time, but the dimension of the X axis keeps intact, leading to a spherical-shaped to a taper-shaped crater because of the Gaussian distribution of the femtosecond laser beam and the spatial lopsided energy deposition of the laser pulses to the material. For the femtosecond laser enhanced wet etching process, the violent interaction, like coulomb explosion between the femtosecond laser and the material, would lead to a localized permanent change of the focal volume and forms a spherical phase or structurally modified region perpendicular to the sample surface. The spatially spherical modified region, which possesses an apparent crater and a surround unapparent phase or structurally modified region as illustrated in Fig. 4(a), is then rapidly etched out by the HF acid and a concave microlens is finally obtained.[20–23] The exposure spots under the same laser influence and the proper tilt angle (40° in our experiment) have the modified regions with similar sizes, which will lead to the microlenses with the low deformation rate after the wet etching process (Fig. S3, supplementary material). However, when the tilt angle is above 50°, the modified regions will differ from each other as less and less laser energy transferred into the material, which will lead to the relatively bigger deformation in the size of the etched microlenses. As shown in Fig. 4(b), after etching 100 min, the dimensions of the Y axis finally approach to the X axis with the angle less than 40°. While the angle is up to 50° and 60°, due to the Gaussian distribution of the femtosecond laser beam, the spatial lopsided energy deposition of the laser pulses would be more and more obvious and results in the size anisotropy of the microlenses. Fig. 4(c) shows the calculated deviations of the microlens individuals via etching time, which demonstrates that the deviation decreased quickly with the etching process. After etching for 100 min, a deviation of individual microlens under 0.5% can be obtained when the angle is less than 40°

(Fig. S4, supplementary material). And the deviation between the microlenses is less than 2% in this condition. So with the efficient incident angle under 40°, we could get high-consistent microlens array via this method.

In conclusion, a low-cost, high-efficient approach involves a femtosecond laser enhanced chemical etching based curved surface micromachining process was presented to directly fabricate omnidirectional concave microlens array on a curved substrate. Then, it was served as a molding template for duplicating bioinspired compound eyes. According to this method, we can obtain the bioinspired compound-eye microlens array with controllable size, high consistency, and low distortion, which show excellent morphology features and fascinating optical performance. In particular, the fabrication process is based on an ordinary 3D translation stage to realize the multidimensional fabrication. Furthermore, if a commercial autofocusing device is introduced in this method, the accuracy and efficiency of this method will be improved significantly. This new method will not only provide a facile and efficient way to fabricate high consistent artificial compound-eye microlens arrays but also reveal some inspirations on fabricating microlens arrays on the complex curved surface by a simple 3D fabrication process.

See supplementary material for more information about the optical microscope images of the concave microlens-in-lens structure, the imaging property of the compound eyes and the deviation of the microlenses via the etching time and the tilt angle.

This work was supported by the National Science Foundation of China (NSFC) (Nos. 61475124, 61275008, 51335008, and 61405154), the Special-funded program on national key scientific instruments and equipment development of China (2012YQ12004706), and China Postdoctoral Science Foundation funded Project (2014M562414). The authors are grateful to the support from the Collaborative Innovation Center of Suzhou Nano Science and Technology and the International Joint Laboratory for Micro/Nano Manufacturing and Measurement Technologies.

[1]L. P. Lee and R. Szema, Science **310**(5751), 1148 (2005).
[2]A. R. Parker and H. E. Townley, Nat. Nanotechnol. **2**(6), 347 (2007).
[3]A. Bruckner, J. Duparre, P. Dannberg, A. Brauer, and A. Tunnermann, Opt. Express **15**(19), 11922 (2007).
[4]K. H. Jeong, J. Kim, and L. P. Lee, Science **312**(5773), 557 (2006).
[5]J. W. Duparre and F. C. Wippermann, Bioinspiration Biomimetics **1**(1), R1 (2006).
[6]X. F. Gao, X. Yan, X. Yao, L. Xu, K. Zhang, J. H. Zhang, B. Yang, and L. Jiang, Adv. Mater. **19**(17), 2213 (2007).
[7]D. Radtke, J. Duparre, U. D. Zeitner, and A. Tunnermann, Opt. Express **15**(6), 3067 (2007).
[8]D. Floreano, R. Pericet-Camara, S. Viollet, F. Ruffier, A. Bruckner, R. Leitel, W. Buss, M. Menouni, F. Expert, R. Juston, M. K. Dobrzynski, G. L'Eplattenier, F. Recktenwald, H. A. Mallot, and N. Franceschini, Proc. Natl. Acad. Sci. U.S.A. **110**(23), 9267 (2013).
[9]C. C. Huang, X. D. Wu, H. W. Liu, B. Aldalali, J. A. Rogers, and H. R. Jiang, Small **10**(15), 3050 (2014).
[10]H. W. Liu, Y. G. Huang, and H. Jiang, Proc. Natl. Acad. Sci. U.S.A. **113**(15), 3982 (2016).
[11]Z. F. Deng, F. Chen, Q. Yang, H. Bian, G. Q. Du, J. L. Yong, C. Shan, and X. Hou, Adv. Funct. Mater. **26**(12), 1995 (2016).
[12]Y. B. Bang, K. M. Lee, and S. Oh, Int. J. Adv. Manuf. Technol. **25**(9–10), 888 (2005).
[13]C. F. Hong, S. Ibaraki, and A. Matsubara, Precis. Eng. **35**(1), 1 (2011).
[14]D. Wu, J. N. Wang, L. G. Niu, X. L. Zhang, S. Z. Wu, Q. D. Chen, L. P. Lee, and H. B. Sun, Adv. Opt. Mater. **2**(8), 751 (2014).
[15]F. Chen, H. W. Liu, Q. Yang, X. H. Wang, C. Hou, H. Bian, W. W. Liang, J. H. Si, and X. Hou, Opt. Express **18**(19), 20334 (2010).
[16]B. Hao, H. W. Liu, F. Chen, Q. Yang, P. B. Qu, G. Q. Du, J. H. Si, X. H. Wang, and X. Hou, Opt. Express **20**(12), 12939 (2012).
[17]F. Chen, Z. F. Deng, Q. Yang, H. Bian, G. Q. Du, J. H. Si, and X. Hou, Opt. Lett. **39**(3), 606 (2014).
[18]H. W. Liu, F. Chen, Q. Yang, P. B. Qu, S. G. He, X. H. Wang, J. H. Si, and X. Hou, Appl. Phys. Lett. **100**(13), 133701 (2012).
[19]P. Nussbaum, R. Volke, H. P. Herzig, M. Eisner, and S. Haselbeck, Pure Appl. Opt. **6**(6), 617 (1997).
[20]A. Marcinkevicius, S. Juodkazis, M. Watanabe, M. Miwa, S. Matsuo, H. Misawa, and J. Nishii, Opt. Lett. **26**(5), 277 (2001).
[21]S. S. Mao, F. Quere, S. Guizard, X. Mao, R. E. Russo, G. Petite, and P. Martin, Appl. Phys. A-Mater. **79**(7), 1695 (2004).
[22]R. R. Gattass and E. Mazur, Nat. Photonics **2**(4), 219 (2008).
[23]K. C. Phillips, H. H. Gandhi, E. Mazur, and S. K. Sundaram, Adv. Opt. Photonics **7**(4), 684 (2015).